

Effective low-energy theory of superconductivity in carbon nanotube ropes

A. De Martino and R. Egger

Institut für Theoretische Physik, Heinrich-Heine-Universität, D-40225 Düsseldorf, Germany

(Dated: October 30, 2018)

We derive and analyze the low-energy theory of superconductivity in carbon nanotube ropes. A rope is modelled as an array of metallic nanotubes, taking into account phonon-mediated as well as Coulomb interactions, and arbitrary Cooper pair hopping amplitudes (Josephson couplings) between different tubes. We use a systematic cumulant expansion to construct the Ginzburg-Landau action including quantum fluctuations. The regime of validity is carefully established, and the effect of phase slips is assessed. Quantum phase slips are shown to cause a depression of the critical temperature T_c below the mean-field value, and a temperature-dependent resistance below T_c . We compare our theoretical results to recent experimental data of Kasumov *et al.* [Phys. Rev. B **68**, 214521 (2003)] for the sub- T_c resistance, and find good agreement with only one free fit parameter. Ropes of nanotubes therefore represent superconductors in the one-dimensional few-channel limit.

PACS numbers: 73.63.Fg, 74.78.Na, 74.25.Fy

I. INTRODUCTION

Over the past decade, the unique mechanical, electrical, and optical properties of carbon nanotubes, including the potential for useful technological applications, have created a lot of excitement [1, 2]. While many of these properties are well understood by now, the experimental observation of intrinsic [3, 4, 5] and anomalously strong proximity-induced [6, 7] superconductivity continues to pose open questions to theoretical understanding. In this paper we present a theory of one-dimensional (1D) superconductivity as found in ropes of carbon nanotubes [3, 4] and potentially in other nanowires. Ropes are 1D materials in the sense that there is only a relatively small number of propagating channels (typically, $N \approx 10$ to 100) available to electronic transport. While most other 1D materials tend to become insulating at low temperatures due to the Peierls transition or as a consequence of electron-electron interactions, nanotubes can stay metallic down to very low temperatures [1]. If the repulsive electron-electron interactions can be overcome by attractive phonon-mediated interactions, ropes of nanotubes can then exhibit a superconducting transition.

However, due to strong 1D fluctuations, this transition is presumably rather broad, and the question of how precisely superconductivity breaks down as the number of propagating channels decreases has to be answered by theory. Experimentally, the breakdown of superconductivity manifests itself as a temperature-dependent resistance below the transition temperature T_c , which becomes more and more pronounced as the rope gets thinner [4]. According to our theory, this resistance is caused by quantum phase slips, and therefore the experimental data published in Ref. [4] have in fact explored a regime of 1D superconductivity with clear evidence for quantum phase slip events that had not been reached before. To the best of our knowledge, nanotube ropes represent wires with the smallest number of propagating channels showing intrinsic superconductivity, even when compared to the amorphous MoGe wires of diameter ≈ 10 nm stud-

ied in Ref. [8], where still several thousand channels are available.

We theoretically analyze superconductivity in nanotube ropes by starting from the microscopic model of an array of N individual metallic single-wall nanotubes (SWNTs) without disorder, with effectively attractive on-tube interactions and inter-tube Josephson couplings. A similar model has been suggested by González [9, 10]. In the absence of the Josephson couplings, each SWNT would then correspond to a *Luttinger liquid* with interaction parameter $g_{c+} > 1$, where $g_{c+} = 1$ marks the non-interacting limit. For simplicity, we take the same g_{c+} on each SWNT. For example, for (10, 10) armchair SWNTs, assuming good screening of the repulsive Coulomb interactions, phonon exchange via a breathing mode (as well as optical phonon modes) leads to $g_{c+} \approx 1.3$, see Ref. [11]. In the case of attractive interactions, the dominant coupling mechanism between different SWNTs is then given by Cooper pair hopping, while single-particle hopping is drastically suppressed by momentum conservation arguments [9, 12]. The coupling among different SWNTs is thus encoded in a *Josephson coupling matrix* Λ_{ij} , where $i, j = 1, \dots, N$. As different nanotube chiralities are randomly distributed in a rope, only 1/3 of the SWNTs can be expected to be metallic. In general, the Λ_{ij} matrix should therefore be drawn from an appropriate random distribution. We consider below one individual rope with a fixed (but unspecified) matrix, and derive general statements valid for arbitrary Λ_{ij} . In that sense, our theory allows to capture some disorder effects, at least qualitatively. However, since typical elastic mean free paths in SWNTs exceed $1\mu\text{m}$ [1], disorder effects within individual SWNTs are ignored completely. The above reasoning leads us to the problem of N coupled strongly correlated Luttinger liquids, where the number of “active” chains $N \lesssim 100$ with reference to the experiments of Ref. [4]. This is a difficult problem that neither permits the use of classical Ginzburg-Landau (GL) theory nor of the standard BCS approach, in contrast to the situation encountered in, e.g., wide quasi-1D organic

superconductors [13].

The approach taken in this paper is sketched next. After a careful derivation of the coupled-chain action in Sec. II, we proceed by introducing the appropriate order parameter field. In Sec. III, we then perform a cumulant expansion in this order parameter, and thereby give a microscopic derivation of the quantum GL action, which then allows to make further progress. We establish the temperature regime where this theory is reliable, and then focus on the important phase fluctuations of the order parameter field. At temperatures T well below a mean-field transition temperature T_c^0 , amplitude fluctuations are shown to be massive, and hence the amplitude can safely be treated in mean-field theory. The massless phase fluctuations then capture the important physics, and we specify the resulting effective low-energy action, valid at temperatures well below T_c^0 . Based on this action, Sec. IV explains why quantum phase slips (QPSs) [14, 15, 16, 17] are crucial for an understanding of the experimental results of Refs. [3, 4]. First, they cause a depression of the transition temperature T_c below the mean-field critical temperature T_c^0 . Furthermore, for $T < T_c$, a finite resistance $R(T)$ due to QPSs appears, which exhibits approximate power-law scaling. We determine the full temperature dependence of $R(T < T_c)$ for arbitrary rope length in Sec. V. In Sec. VI, we then compare these results for $R(T)$ to the experimental data of Ref. [4], focussing on two of their samples. Finally, Sec. VII offers some concluding remarks. Throughout the paper, we put $\hbar = k_B = 1$.

II. MODEL AND ORDER PARAMETER

We consider a rope consisting of N metallic SWNTs participating in superconductivity. Experimentally, this number can be found from the residual resistance measured as offset in the resistance when extrapolating down to $T = 0$ [4]. Due to the attached normal electrodes in any two-terminal measurement of the rope, despite of the presence of superconductivity, there will always be a finite contact resistance R_c . Since each metallic tube contributes two conduction channels, assuming good transparency for the contacts between metallic tubes and the electrodes, this is given by

$$R_c = \frac{R_Q}{2N}, \quad R_Q = h/2e^2 \simeq 12.9 k\Omega. \quad (2.1)$$

Extrapolation of experimental data for the resistance $R(T)$ down to $T \rightarrow 0$ within the superconducting regime then allows to measure R_c , and hence N . Good transparency of the contacts is warranted by the sputtering technique used to fabricate and contact the suspended rope samples in the experiments of Refs. [3, 4]. An alternative way to estimate N comes from atomic force microscopy, which allows to measure the apparent radius of the rope, and hence yields an estimate for the total number of tubes in the rope. On average, 1/3 of the

tubes are metallic [1], and one should obtain the same number N from this approach. Fortunately, these two ways of estimating N provide consistent results in most samples [4]. Therefore the values for N used below are expected to be reliable.

Here we always assume that phonon exchange leads to attractive interactions overcoming the (screened) Coulomb interactions. This assumption can be problematic in ultrathin ropes, where practically no screening arises unless there are close-by gate electrodes. For sufficiently large rope radius, however, theoretical arguments supporting this scenario have been provided in Ref. [18]. In the absence of intra-tube disorder, then the appropriate low-energy theory for an individual SWNT is the Luttinger liquid (LL) model [11, 19, 20]. The LL theory of SWNTs is usually formulated within the Abelian bosonization approach [21]. With $\mathbf{x} = (x, \tau)$, where x is the spatial 1D coordinate along the tube, and $0 \leq \tau < 1/T$ is imaginary time, and corresponding integration measure $d\mathbf{x} = dx d\tau$, the action for a single SWNT is [11, 19, 20]

$$\begin{aligned} S_{\text{LL}} &= \int d\mathbf{x} \sum_{a=c\pm, s\pm} \frac{v_a}{2g_a} [(\partial_\tau \varphi_a/v_a)^2 + (\partial_x \varphi_a)^2] \\ &= \int d\mathbf{x} \sum_a \frac{v_a g_a}{2} [(\partial_\tau \theta_a/v_a)^2 + (\partial_x \theta_a)^2], \quad (2.2) \end{aligned}$$

which we take to be the same for every SWNT. Due to the electron spin and the additional K point degeneracy present in nanotubes [1], there are four channels, $a = c+, c-, s+, s-$, corresponding to the total/relative charge/spin modes [19, 20], with associated boson fields $\varphi_a(\mathbf{x})$ and dual fields $\theta_a(\mathbf{x})$ [21]. In the $a = (c+, s-)$ channels, the second (dual) formulation turns out to be more convenient, while the first line of Eq. (2.2) is more useful for $a = (s+, c-)$. The combined effect of Coulomb and phonon-mediated electron-electron interactions results in the interaction parameter g_{c+} , where we assume $g_{c+} > 1$, reflecting effectively attractive interactions [11]. In the neutral channels, there are only very weak residual interactions, and we therefore put $g_{a \neq c+} = 1$. Finally, the velocities v_a in Eq. (2.2) are defined as $v_a = v_F/g_a$, where $v_F = 8 \times 10^5$ m/sec is the Fermi velocity.

Next we address the question which processes trigger the strongest superconducting fluctuations in a nanotube rope. This question has been addressed in Refs. [9, 10, 11], and the conclusion of these studies is that Cooper pairs predominantly form on individual SWNTs rather than involving electrons on different SWNTs, see, e.g., the last section in Ref. [11] for a detailed discussion. Furthermore, the dominant intra-tube fluctuations involve *singlet* (rather than triplet) Cooper pairs. The relevant order parameter for superconductivity is then given by [22]

$$\mathcal{O}(\mathbf{x}) = \sum_{r\sigma\beta} \sigma \psi_{r,\sigma,\beta}(\mathbf{x}) \psi_{-r,-\sigma,-\beta}(\mathbf{x}), \quad (2.3)$$

where $\psi_{r\sigma\beta}$ denotes the electron field operator for a right- or left-moving electron ($r = \pm$) with spin $\sigma = \pm$ and K point degeneracy index $\beta = \pm$. In bosonized language, this operator can be expressed as [22]

$$\begin{aligned} \mathcal{O} &= \frac{1}{\pi a_0} \cos[\sqrt{\pi}\theta_{c+}] \cos[\sqrt{\pi}\varphi_{c-}] \\ &\times \cos[\sqrt{\pi}\varphi_{s+}] \cos[\sqrt{\pi}\theta_{s-}] - (\cos \leftrightarrow \sin), \end{aligned} \quad (2.4)$$

where we identify the UV cutoff necessary in the bosonization scheme with the graphite lattice constant, $a_0 = 0.24$ nm. In what follows, we use the shorthand notation φ_j to label all four boson fields φ_a (or their dual fields) corresponding to the j th SWNT, where $j = 1, \dots, N$.

The next step is to look at possible couplings among the individual SWNTs. In principle, three different processes should be taken into account, namely (i) direct Coulomb interactions, (ii) Josephson couplings, and (iii) single-electron hopping. The last process is strongly suppressed due to the generally different chirality of adjacent tubes [12], and, in addition, for $g_{c+} > 1$, inter-SWNT Coulomb interactions are irrelevant [13]. Furthermore, as discussed in detail in Ref. [11], phonon-exchange mediated interactions between *different* SWNTs can always be neglected against the intra-tube interactions. Therefore the most relevant mechanism is Josephson coupling between metallic SWNTs. These couplings define a Josephson matrix Λ_{jk} , which contains the amplitudes for Cooper pair hopping from the j th to the k th SWNT. We put $\Lambda_{jj} = 0$, and hence Λ is a real, symmetric, and traceless matrix. It therefore has only real eigenvalues Λ_α , which we take in descending order, $\Lambda_1 \geq \Lambda_2 \geq \dots \geq \Lambda_N$. Moreover, there is at least one positive and at least one negative eigenvalue. The largest eigenvalue Λ_1 will be shown to determine the mean-field critical temperature T_c^0 below. The matrix Λ is then expressed in the corresponding orthonormal eigenbasis $|\alpha\rangle$,

$$\Lambda_{jk} = \sum_{\alpha} \langle j|\alpha\rangle \Lambda_{\alpha} \langle \alpha|k\rangle, \quad (2.5)$$

where $\langle j|\alpha\rangle$ is the real orthogonal transformation from the basis of lattice points $\{|j\rangle\}$ to the basis $\{|\alpha\rangle\}$ that diagonalizes Λ . Clearly, $\langle j|\alpha\rangle = \langle \alpha|j\rangle$. In what follows, we define α_0 such that $\Lambda_{\alpha} > 0$ for $\alpha < \alpha_0$.

The Euclidean action of the rope is then

$$S = \sum_{j=1}^N S_{LL}[\varphi_j] - \sum_{jk} \Lambda_{jk} \int d\mathbf{x} \mathcal{O}_j^* \mathcal{O}_k, \quad (2.6)$$

where \mathcal{O}_j is the order parameter specified in Eq. (2.4). The action (2.6) defines the model that is studied in the remainder of our paper. For studies of closely related models, see also Refs. [13, 23].

In order to decouple the Josephson term in Eq. (2.6), we employ a Hubbard-Stratonovich transformation. To that purpose, since the Josephson matrix has at least one

negative eigenvalue, we first express Λ in its eigenbasis, see Eq. (2.5). The Josephson term in Eq. (2.2) is then rewritten as

$$\sum_{jk} \mathcal{O}_j^* \Lambda_{jk} \mathcal{O}_k = \sum_{\alpha} \text{sgn}(\Lambda_{\alpha}) |\Lambda_{\alpha}| \mathcal{O}_{\alpha}^* \mathcal{O}_{\alpha},$$

where the order parameter in the $|\alpha\rangle$ basis is

$$\mathcal{O}_{\alpha} \equiv \sum_i \langle \alpha|i\rangle \mathcal{O}_i, \quad \mathcal{O}_{\alpha}^* \equiv \sum_i \mathcal{O}_i^* \langle i|\alpha\rangle. \quad (2.7)$$

By introducing a field $\Delta_{\alpha}(\mathbf{x})$ for each Josephson eigenmode [24], with (formally independent) complex conjugate field Δ_{α}^* , it is now possible to perform the Hubbard-Stratonovich transformation following the standard procedure [25]. With integration measure $\mathcal{D}\Delta = \prod_{\alpha} \mathcal{D}\Delta_{\alpha}^* \mathcal{D}\Delta_{\alpha}$, the effective action entering the partition function $Z = \int \mathcal{D}\Delta \exp(-S_{\text{eff}}[\Delta])$ reads

$$S_{\text{eff}}[\Delta] = S_0[\Delta] + \int d\mathbf{x} \sum_{\alpha} \Delta_{\alpha}^* \frac{1}{|\Lambda_{\alpha}|} \Delta_{\alpha}, \quad (2.8)$$

where the action $S_0[\Delta]$ is formally defined via the remaining path integral over the boson fields φ_j ,

$$\begin{aligned} S_0[\Delta] &= -\ln \int \prod_{j=1}^N \mathcal{D}\varphi_j e^{-\sum_j S_{LL}[\varphi_j]} \times \\ &\times e^{-\int d\mathbf{x} \sum_{\alpha} c_{\alpha} (\Delta_{\alpha}^* \mathcal{O}_{\alpha} + \mathcal{O}_{\alpha}^* \Delta_{\alpha})}, \end{aligned} \quad (2.9)$$

with $c_{\alpha} = 1$ for $\alpha < \alpha_0$, and $c_{\alpha} = i$ otherwise.

III. QUANTUM GINZBURG-LANDAU APPROACH

A. Cumulant expansion

Clearly, closed analytical evaluation of the path integral in Eq. (2.9) is in general impossible. In order to make progress, approximations are necessary, and in the following we shall construct and analyze the Ginzburg-Landau (GL) action [14, 25] for this problem. It turns out to be essential to take into account quantum fluctuations, i.e., the imaginary-time dependence of the order parameter field $\Delta_{\alpha}(x, \tau)$. In the standard (static) Ginzburg-Landau theory, such effects are ignored.

The derivation of the GL action proceeds from a cumulant expansion of Eq. (2.9) up to quartic order in the Δ_{α} . This is a systematic expansion in the parameter $|\Delta|/2\pi T$ [25], and by self-consistently computing this parameter, one can determine the regime of validity of GL theory. We stress that this expansion is *not* restricted to $N \gg 1$. In addition, for the long-wavelength low-energy regime of primary interest here, we are entitled to perform a gradient expansion. Using the single-chain correlation function $G(\mathbf{x}_{12}) = \langle \mathcal{O}(\mathbf{x}_1) \mathcal{O}^*(\mathbf{x}_2) \rangle$ of the operator \mathcal{O} in

Eq. (2.4) with respect to the free boson action S_{LL} , and the connected four-point correlation function

$$\begin{aligned} G_c^{(4)}(\mathbf{x}_1, \mathbf{x}_2, \mathbf{x}_3, \mathbf{x}_4) &= \langle \mathcal{O}(\mathbf{x}_1) \mathcal{O}(\mathbf{x}_2) \mathcal{O}^*(\mathbf{x}_3) \mathcal{O}^*(\mathbf{x}_4) \rangle \\ &\quad - \langle \mathcal{O}(\mathbf{x}_1) \mathcal{O}^*(\mathbf{x}_3) \rangle \langle \mathcal{O}(\mathbf{x}_2) \mathcal{O}^*(\mathbf{x}_4) \rangle \\ &\quad - \langle \mathcal{O}(\mathbf{x}_1) \mathcal{O}^*(\mathbf{x}_4) \rangle \langle \mathcal{O}(\mathbf{x}_2) \mathcal{O}^*(\mathbf{x}_3) \rangle, \end{aligned}$$

the cumulant-plus-gradient expansion up to quartic order yields for the effective Lagrangian density

$$\begin{aligned} L[\Delta] &= \sum_{\alpha < \alpha_0} \left[C |\partial_x \Delta_\alpha|^2 + D |\partial_\tau \Delta_\alpha|^2 \right. \\ &\quad \left. + (\Lambda_\alpha^{-1} - A) |\Delta_\alpha|^2 \right] \\ &\quad + B \sum_{\alpha_i < \alpha_0} f_{\alpha_3, \alpha_4}^{\alpha_1, \alpha_2} \Delta_{\alpha_1}^* \Delta_{\alpha_2}^* \Delta_{\alpha_3} \Delta_{\alpha_4}, \end{aligned} \quad (3.1)$$

where we use the notation

$$f_{\alpha_3, \alpha_4}^{\alpha_1, \alpha_2} = \sum_i \langle \alpha_1 | i \rangle \langle \alpha_2 | i \rangle \langle i | \alpha_3 \rangle \langle i | \alpha_4 \rangle.$$

The temperature-dependent positive coefficients A, B, C, D are obtained as

$$A = \int d\mathbf{x} G(\mathbf{x}), \quad (3.2)$$

$$B = -\frac{1}{4} \int d\mathbf{x}_1 d\mathbf{x}_2 d\mathbf{x}_3 G_c^{(4)}(\mathbf{x}_1, \mathbf{x}_2, \mathbf{x}_3, \mathbf{x}_4), \quad (3.3)$$

$$C = \frac{1}{2} \int d\mathbf{x} x^2 G(\mathbf{x}), \quad (3.4)$$

$$D = \frac{1}{2} \int d\mathbf{x} \tau^2 G(\mathbf{x}). \quad (3.5)$$

Due to translation invariance, the integral for B does not depend on \mathbf{x}_4 . Besides temperature, these coefficients basically depend only on the important LL interaction parameter g_{c+} . In particular, as it is discussed below, for $g_{c+} > 1$, the coefficient A grows as T is lowered. For static and uniform configurations, modes with $\alpha > \alpha_0$ never become critical. One can then safely integrate over these modes, which leads to a renormalization of the parameters governing the remaining modes. Such renormalization effects are however tiny, and thus are completely neglected in Eq. (3.1).

At this stage, it is useful to switch to an order parameter field defined on the j th SWNT,

$$\Delta_j = \sum_{\alpha < \alpha_0} \langle j | \alpha \rangle \Delta_\alpha. \quad (3.6)$$

After some algebra, the Lagrangian density (3.1) can be written as

$$\begin{aligned} L[\Delta] &= \sum_{j=1}^N \left[C |\partial_x \Delta_j|^2 + D |\partial_\tau \Delta_j|^2 + B |\Delta_j|^4 + \right. \\ &\quad \left. + (\Lambda_1^{-1} - A) |\Delta_j|^2 \right] + \sum_{jk} \Delta_j^* V_{jk} \Delta_k, \end{aligned} \quad (3.7)$$

with the real, symmetric, and positive definite matrix

$$V_{jk} = \sum_{\alpha < \alpha_0} \langle j | \alpha \rangle (\Lambda_\alpha^{-1} - \Lambda_1^{-1}) \langle \alpha | k \rangle. \quad (3.8)$$

Notice that, strictly speaking, the fields Δ_i are not all independent, because we have defined them from the subset of positive modes. The transformation in Eq. (3.6) is indeed not invertible. Nevertheless, in the following, we treat them as formally independent. This only affects the precise values of the V_{ij} but does not qualitatively change our results. The expectation value of the order parameter field (2.4) can be expressed in terms of linear combinations of the fields $\Delta_j(x, \tau)$, and hence it is indeed justified to call Δ_j a proper ‘‘order parameter field’’.

Equation (3.7) specifies the full GL action, taking into account quantum fluctuations and transverse modes for arbitrary number N of active SWNTs. In the limit $N \rightarrow \infty$, and considering only static field configurations, results similar to those of Ref. [13] are recovered. In that limit the last term in Eq. (3.7) gives indeed the gradient term in the transverse direction, and one obtains the standard 3D GL Lagrangian. There is however an important difference, namely the starting point of Ref. [13] is a model of Josephson-coupled 1D superconductors, whereas we start from an array of metallic chains with $g_{c+} > 1$, where the inter-chain Josephson coupling is crucial in stabilizing superconductivity. More similar to ours is the model investigated in Ref. [23]. However, in that paper, the metallic chains are assumed to have a spin gap, which is not the case for the SWNTs in a rope in the temperature range of interest. Furthermore, the main focus in Ref. [23] is the competition between charge density wave and superconducting instabilities, whereas in our case, as discussed above, the formation of a charge density wave is strongly suppressed by compositional disorder, i.e., different chiralities of adjacent tubes, and we do not have to take the corresponding instability into account.

B. Ginzburg-Landau coefficients

In order to make quantitative predictions, it is necessary to compute the GL coefficients defined in Eqs.(3.2)-(3.5). While this is possible in principle for the full four-channel model (2.2), here we will instead derive the coefficients for a simpler model, where the K point degeneracy is neglected. This leads to an effective spin-1/2 Luttinger liquid action with interaction parameter g_c ($g_s = 1$) and velocity $v_c = v_F/g_c$ ($v_s = v_F$). Up to a prefactor of order unity, the respective results can be matched onto each other. This can be made explicit, e.g., for the coefficient A , where we get from the full action (2.2)

$$A = \frac{c}{v_F} \left(\frac{\pi a_0 T}{v_{c+}} \right)^{(g_{c+}^{-1} - 1)/2}.$$

The proportionality constant c is found to differ from $\tilde{A}/2\pi^2$ [see Eq. (3.9) below, which follows from the spin-

1/2 description] only by a factor of order unity. In the simpler model neglecting the K point degeneracy, one then needs to take

$$g_c^{-1} = \frac{1 + g_{c+}^{-1}}{2},$$

which gives, for $g_{c+} = 1.3$, a value of $g_c \approx 1.1$. This way, all exponents of the resulting power-law correlation functions (which are the physically relevant quantities) in the ‘‘reduced’’ model are the same as in the complete model, and only prefactors of order unity may be different for the respective GL coefficients. The bosonized order parameter (2.4) in the simpler model is then given by

$$\mathcal{O} = \frac{1}{\pi a_0} \cos[\sqrt{2\pi}\varphi_s] \exp[i\sqrt{2\pi}\theta_c].$$

Using the finite-temperature correlation functions of the fields θ_c and φ_s [21],

$$\begin{aligned} \langle \theta_c(\mathbf{x})\theta_c(\mathbf{0}) \rangle &= \frac{-1}{2\pi g_c} \ln \left(\frac{v_c}{\pi a_0 T} \left| \sinh \frac{\pi T(x + iv_c\tau)}{v_c} \right| \right), \\ \langle \varphi_s(\mathbf{x})\varphi_s(\mathbf{0}) \rangle &= \frac{-1}{2\pi} \ln \left(\frac{v_F}{\pi a_0 T} \left| \sinh \frac{\pi T(x + iv_F\tau)}{v_F} \right| \right), \end{aligned}$$

and rescaling the integration variables x and τ in Eqs. (3.2)-(3.5), explicit expressions follow in the form

$$\begin{aligned} A(T) &= \frac{1}{2\pi^2 v_F} (\pi a_0 T / v_c)^{g_c^{-1}-1} \tilde{A}, \\ B(T) &= \frac{a_0^2}{32\pi^4 v_c v_F^2} (\pi a_0 T / v_c)^{2g_c^{-1}-4} \tilde{B}, \\ C(T) &= \frac{a_0^2}{4\pi^2 v_F} (\pi a_0 T / v_c)^{g_c^{-1}-3} \tilde{C}, \\ D(T) &= \frac{a_0^2}{4\pi^2 v_F v_c^2} (\pi a_0 T / v_c)^{g_c^{-1}-3} \tilde{D}. \end{aligned} \quad (3.9)$$

Dimensionless g_c -dependent numbers $\tilde{A}, \tilde{B}, \tilde{C}, \tilde{D}$ were defined as follows. With the notation $\mathbf{z} = (w, u)$ and

$$\int d\mathbf{z} = \int_0^\pi du \int_{-\infty}^\infty dw,$$

we have

$$\begin{aligned} \tilde{A} &= \int \frac{d\mathbf{z}}{f_c(\mathbf{z})f_s(\mathbf{z})}, \\ \tilde{C} &= \int d\mathbf{z} \frac{w^2}{f_c(\mathbf{z})f_s(\mathbf{z})}, \\ \tilde{D} &= \int d\mathbf{z} \frac{u^2}{f_c(\mathbf{z})f_s(\mathbf{z})}, \end{aligned}$$

where functions $f_{c,s}$ are introduced as

$$\begin{aligned} f_c(\mathbf{z}) &= |\sinh(w + iu)|^{1/g_c}, \\ f_s(\mathbf{z}) &= |\sinh(w/g_c + iu)|. \end{aligned}$$

The coefficient of the quartic term in the GL functional is

$$\begin{aligned} \tilde{B} &= \int \frac{d\mathbf{z}_1 d\mathbf{z}_2 d\mathbf{z}_3}{f_c(\mathbf{z}_2)f_c(\mathbf{z}_{13})} \left[\frac{4}{f_s(\mathbf{z}_2)f_s(\mathbf{z}_{13})} - \frac{f_c(\mathbf{z}_1)f_c(\mathbf{z}_{23})}{f_c(\mathbf{z}_3)f_c(\mathbf{z}_{12})} \right] \\ &\times \left(\frac{f_s(\mathbf{z}_1)f_s(\mathbf{z}_{23})}{f_s(\mathbf{z}_2)f_s(\mathbf{z}_{13})f_s(\mathbf{z}_3)f_s(\mathbf{z}_{12})} + (1 \leftrightarrow 2) + (1 \leftrightarrow 3) \right) \end{aligned}$$

with $\mathbf{z}_{ij} = (w_i - w_j, u_i - u_j)$. The quantity \tilde{B} is evaluated using the Monte Carlo method. For $g_c = 1$, we first numerically reproduced the exact result $\tilde{B} = 8\pi^2 \tilde{C}$ with $\tilde{C} = 7\pi\zeta(3)/4$ [25]. Numerical values can then be obtained for arbitrary g_c . Numerical evaluation yields for $g_c \approx 1.1$ (corresponding to $g_{c+} = 1.3$) the following results:

$$\tilde{A} \simeq 17.4, \quad \tilde{B} \simeq 392(1), \quad \tilde{C} \simeq 8.15, \quad \tilde{D} \simeq 6.97. \quad (3.10)$$

C. Mean-field transition temperature

Since in the rope only a modest number of transverse modes are present, a natural definition of the mean-field critical temperature T_c^0 is the temperature at which the mode corresponding to the largest eigenvalue of Λ becomes critical. From Eq. (3.7), this leads to the condition $A(T) = \Lambda_1^{-1}$, and hence to the mean-field critical temperature

$$T_c^0 = \frac{v_c}{\pi a_0} \left(\frac{\tilde{A}\Lambda_1}{2\pi^2 v_F} \right)^{g_c/(g_c-1)}, \quad (3.11)$$

which exhibits a dependence on the number N of active SWNTs in the rope through Λ_1 . For large N , the eigenvalue Λ_1 saturates, and Eq. (3.11) approaches the bulk transition temperature.

To provide concrete theoretical predictions for T_c^0 is difficult, since the Josephson matrix is in general unknown, and the results for T_c^0 very sensitively depend on Λ_1 . Using estimates of Ref. [10] and typical N as reported in Ref. [4], as an order-of-magnitude estimate, we find T_c^0 values around 0.1 to 1 K. When comparing to experimental results, Λ_1 can be inferred from the actually measured T_c , which in turn provides values in reasonable agreement with theoretical expectations [9].

D. Low-energy theory: $T < T_c^0$

In what follows, we focus on temperatures $T < T_c^0$. Then it is useful to employ an amplitude-phase representation of the order parameter field,

$$\Delta_j(\mathbf{x}) = |\Delta_j| \exp[i\phi_j(\mathbf{x})], \quad (3.12)$$

where the amplitudes $|\Delta_j|$ are expected to be finite with a gap for fluctuations around their mean-field value. At

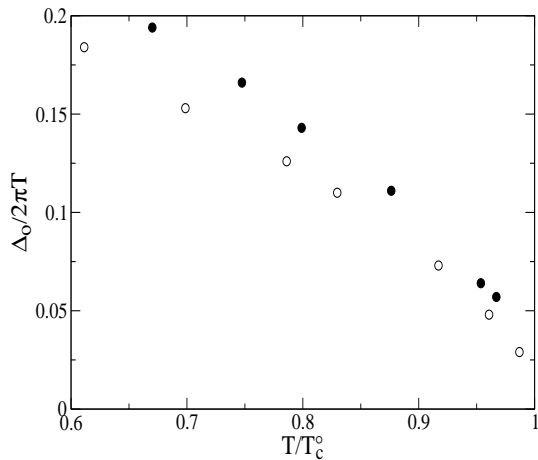


FIG. 1: Temperature dependence of $\Delta_0/2\pi T$ versus T/T_c^0 for $N = 31$ (open circles) and $N = 253$ (filled circles).

not too low temperatures, the GL action corresponding to Eq. (3.7) is accurate (see below), and the mean-field values follow from the saddle-point equations. Considering only static and uniform field configurations, we find $\phi_i \equiv \phi$, where in principle also other (frustrated) configurations with $\phi_i - \phi_j = \pm\pi$ could contribute. Such configurations presumably correspond to maxima of the free energy, and are ignored henceforth. The saddle-point equations then reduce to equations for the amplitudes alone,

$$\sum_j V_{ij} |\Delta_j| + (\Lambda_1^{-1} - A) |\Delta_i| + 2B |\Delta_i|^3 = 0, \quad (3.13)$$

whose solution yields the transverse order parameter profile. Numerical study of Eq. (3.13) using a standard Newton-Raphson root-finding algorithm then allows to extract the profile $\{|\Delta_j|\}$ for a given Josephson matrix Λ_{ij} . We briefly discuss the solution of Eq. (3.13) for the idealized model of a rope as a trigonal lattice exclusively composed of N metallic SWNTs, where $\Lambda_{ij} = \lambda$ for nearest neighbors (i, j) , and $\Lambda_{ij} = 0$ otherwise. For this model, Fig. 1 shows the resulting average amplitude $\Delta_0 = \sum_i |\Delta_i|/N$ as a function of temperature for $\lambda/v_F = 0.1$ and two values of N . Since $\Delta_0/2\pi T$ is the expansion parameter entering the construction of the GL functional, and it remains small down to $T \approx T_c^0/2$, we conclude that the GL theory is self-consistently valid in a quantitative way down to such temperature scales. In our discussion below, GL theory turns out to be qualitatively useful even down to $T = 0$.

Fixing the amplitudes $|\Delta_j|$ at their mean-field values, and neglecting the massive amplitude fluctuations around these values, the Lagrangian follows from

Eq. (3.7) as

$$L = \sum_{j=1}^N \frac{\mu_j}{2\pi} [c_s (\partial_x \phi_j)^2 + c_s^{-1} (\partial_\tau \phi_j)^2] + \sum_{i>j} 2V_{ij} |\Delta_i| |\Delta_j| \cos(\phi_i - \phi_j), \quad (3.14)$$

with the Mooij-Schön velocity [26],

$$c_s \equiv v_c \sqrt{\tilde{C}/\tilde{D}}, \quad (3.15)$$

and dimensionless phase stiffness parameters

$$\mu_j = 2\pi C |\Delta_j|^2 / c_s. \quad (3.16)$$

At this stage, electromagnetic potentials can be coupled in via standard Peierls substitution rule [25], and dissipative effects due to the electromagnetic environment can be incorporated following Ref. [17].

IV. 1D ACTION AND QUANTUM PHASE SLIPS

A. 1D phase action

Numerical evaluation of Eq. (3.13) shows that for T well below T_c^0 , transverse fluctuations are heavily suppressed. While this statement only applies to amplitude fluctuations, one can argue that also the transverse phase fluctuations are strongly suppressed. The basic argument relates to the scaling dimension [in the renormalization group (RG) sense] of the operator $\cos(\phi_i - \phi_j)$, which is essentially governed by the μ_j . For T well below T_c^0 , the μ_j become large, and the cosine operators get strongly relevant, locking the phases all together. In the low-temperature regime of main interest below, this argument allows to substantially simplify Eq. (3.14). Then also no detailed knowledge about the Josephson matrix is required, because the only relevant information is essentially contained in T_c^0 .

Putting all phases $\phi_j = \phi$, we arrive at a standard (Gaussian) 1D superconducting phase action [14],

$$S = \frac{\mu}{2\pi} \int dx d\tau [c_s^{-1} (\partial_\tau \phi)^2 + c_s (\partial_x \phi)^2], \quad (4.1)$$

with dimensionless rigidity $\mu = \sum_j \mu_j$, see Eq. (3.16), and c_s as given in Eq. (3.15). Assuming GL theory to work even down to $T = 0$ for the moment, and neglecting the V_{ij} -term in Eq. (3.13), a simple analytical estimate follows in the form

$$\mu(T) = N\nu \left[1 - (T/T_c^0)^{(g_c-1)/g_c} \right], \quad (4.2)$$

where the number ν is

$$\nu = 4\pi \tilde{A} (\tilde{C}\tilde{D})^{1/2} / \tilde{B}. \quad (4.3)$$

The peculiar temperature dependence of the phase stiffness in Eq. (4.2), reflecting the underlying LL physics of the individual SWNTs, is one of the main results of this paper. In the effective spin-1/2 description employed here, using the numbers specified in Eq. (3.10) for $g_c = 1.1$ results in $\nu \approx 4$. Remarkably, at $T = 0$, Eq. (4.2) coincides, up to a prefactor of order unity, with the rigidity $\bar{\mu}$ obtained from standard mean-field relations [25],

$$\bar{\mu} = \pi^2 n_s R^2 / 2m^* c_s = \bar{\nu} N.$$

With the density of condensed electrons n_s and rope radius R , this implies $\bar{\nu} \approx v_F/c_s$, which is of order unity. We therefore conclude that the GL prediction (4.2) for $\mu(T)$ is robust and useful even outside its strict validity regime.

The result (4.2) for the stiffness is central for the following discussion. The value we obtain for ν , however, should not be taken as a very precise estimate. First, it can be affected by factors of order unity under a full four-channel calculation taking into account the K point degeneracy, as this affects each of the numbers in Eq. (3.10) by a factor of order unity. Second, uncertainties in the parameter g_c will also affect ν by a factor of order unity. Moreover, based on the discussion in Ref. [16], one expects on general grounds that intra-SWNT disorder and dissipative effects, both of which are not included in our model, will effectively lead to a *decrease* of the parameter ν entering Eq. (4.2). Therefore ν is taken below as a fit parameter when comparing to experimental data. Since the number of active SWNTs N can be estimated from the residual resistance, and the transition temperature T_c , see Eq. (4.7) below, can be determined from the experimentally observed transition temperature, ν is basically the only free remaining parameter. Fits of our theoretical results to experimental data are then expected to yield values for ν around $\nu \approx 1$. This is verified below in Sec. VI.

B. Phase slips

In the 1D situation encountered here, superconductivity can be destroyed by phase slips [14]. A phase slip (PS) can be visualized as a process in which fluctuations locally destroy the amplitude of the superconducting order parameter, which effectively disconnects the 1D superconductor into two parts. Simultaneously, the phase, being defined only up to 2π , is allowed to “slip” by 2π across the region where the amplitude vanishes. This process then leads to finite dissipation in the superconducting wire via the Josephson effect. Depending on temperature, phase slips can be produced either by thermal or by quantum fluctuations. In the first case, which is commonly realized very near the critical temperature, we have a thermally activated phase slip (TAPS). At lower temperature, the quantum tunneling mechanism dominates, and one speaks of a quantum phase slip (QPS).

For a textbook description of quantum phase slips, see Ref. [27]. Below we demonstrate that in superconducting ropes, only QPSs are expected to play a prominent role.

A QPS is a topological vortex-like excitation of the superconducting phase field $\phi(x, \tau)$ that solves the equation of motion for the action (4.1) with a singularity at the core, where superconducting order is locally destroyed and a phase cannot be defined. Defining a thermal lengthscale as

$$L_T = c_s / \pi T, \quad (4.4)$$

for rope length $L \rightarrow \infty$ and $L_T \rightarrow \infty$, a QPS with core at (x_i, τ_i) and winding number $k_i = \pm 1$ (higher winding numbers are irrelevant) is given by [27]

$$\phi(x, \tau) = k_i \arctan \left[\frac{c_s(\tau - \tau_i)}{(x - x_i)} \right], \quad (4.5)$$

where the finite L, L_T solution follows by conformal transformation [17]. The action of a QPS consists of two terms, one associated with the local loss of condensation energy, the core action S_c , and the other with the vortex strain energy. While a detailed computation of S_c requires a microscopic description of the dynamics inside the vortex core [16], a simple qualitative argument is able to predict an order-of-magnitude estimate $S_c \approx \mu/2$ [27].

This result allows us to assess the relative contribution of the TAPS and QPS mechanisms. The production rate for the creation of one vortex is [16] $\gamma_{\text{QPS}} \approx \frac{S_c L c_s}{\kappa} \exp(-S_c)$, where κ is the core size. Within exponential accuracy, comparing this formula to the respective standard TAPS rate expression [14], the crossover temperature from TAPS- to QPS-dominated behavior is $T_{\text{PS}}^* = 2\Delta F / N\nu$, with activation barrier ΔF . Using results of Ref. [23], we estimate the latter as $\Delta F = 8\sqrt{2}R(g_c)NT_c^0/3$, with dimensionless coefficient $R(g_c)$ of order unity. Finally, this implies $T_{\text{PS}}^* \approx T_c^0$. Since the true transition temperature $T_c < T_c^0$, see below, in the temperature regime $T < T_c$, the influence of a TAPS can safely be neglected against the QPS.

The generalization to many QPSs then leads to the standard picture of a Coulomb gas of charges $k_i = \pm 1$, with fugacity $y = e^{-S_c}$, total charge zero, and logarithmic interactions [25, 27]. The partition function $Z = Z_G Z_V$ contains a regular factor Z_G and the vortex contribution

$$Z_V = \sum_{n=0}^{\infty} \frac{y^{2n}}{(n!)^2} \int \frac{\prod_{m=1}^{2n} d\mathbf{r}_m}{(c_s \kappa^2)^{2n}} \sum_{\{k\}} e^{\mu \sum_{i \neq j} k_i k_j \ln(r_{ij}/\kappa)}. \quad (4.6)$$

This model undergoes a Berezinski-Kosterlitz-Thouless transition driven by the nucleation of vortices, here corresponding to a transition from a phase $\mu > \mu^*$, where QPSs are confined into neutral pairs and the rope forms a 1D superconductor with finite phase stiffness and quasi-long-range order, to a phase $\mu < \mu^*$ where QPSs proliferate. In that phase, vortices are deconfined and destroy

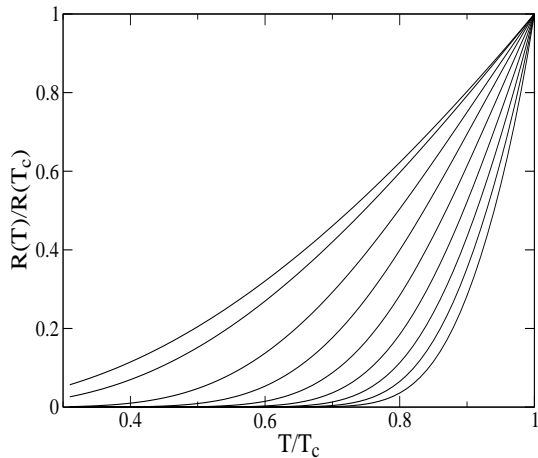


FIG. 2: Temperature-dependent resistance $R(T < T_c)$ predicted by Eq. (5.4) for $\nu = 1$ and different N . The smaller is N , the broader is the transition. From the leftmost to the rightmost curve, $N = 4, 7, 19, 37, 61, 91, 127, 169, 217$.

the phase stiffness, thereby producing normal behavior, where “normal” does of course not imply Fermi-liquid behavior. The phase boundary is located at $\mu^* = 2 + 4\pi y \simeq 2$. The true transition temperature T_c is therefore *not* the mean-field transition temperature T_c^0 , but follows from the condition $\mu(T_c) = \mu^*$. Putting $\mu^* = 2$, Eq. (4.2) yields

$$T_c/T_c^0 = [1 - 2/N\nu]^{g_c/(g_c-1)}. \quad (4.7)$$

This T_c depression is quite sizeable for $N \lesssim 100$. To give concrete numbers, taking $\nu = 1$, for $N = 25, 50$, and 100 , the ratio T_c/T_c^0 equals $0.40, 0.63$, and 0.80 , respectively. QPSs also have an important and observable effect in the superconducting regime, as will be discussed in the next section.

V. RESISTANCE BELOW T_c

A phase slip produces finite dissipation through the Josephson effect, and therefore introduces a finite resistance even in the superconducting state, $T < T_c$. The QPS-induced linear resistance $R(T) = V/I$ for $T < T_c$ can be computed perturbatively in the QPS fugacity y [15]. For that purpose, we imagine that one imposes a small current I to flow through the rope. The presence of QPSs implies that a voltage drop V occurs, which is related to the average change in phase,

$$V = \frac{\langle \dot{\phi} \rangle}{2e} = \frac{\pi}{e} [\Gamma(I) - \Gamma(-I)],$$

where $\Gamma(\pm I)$ is the rate for a phase slip by $\pm 2\pi$ [15]. This rate can be obtained following Langer [28] as the imaginary part acquired by the free energy $F(I)$ under an appropriate analytic continuation,

$$\Gamma(\pm I) = -2 \operatorname{Im} F(\pm I). \quad (5.1)$$

We only consider the contribution of a single pair of QPSs, i.e., compute $R(T)$ to second order in y . Expanding Eq. (4.6) to order y^2 , the free energy at this order reads

$$F = -\frac{Ly^2c_s^2}{\kappa^4} \int_0^{1/T} d\tau \int_{-L/2}^{L/2} dx e^{\epsilon\tau - 2\mu g_E(x,\tau)}, \quad (5.2)$$

where the vortex-vortex interaction $g_E(x,\tau)$ only depends on relative coordinates, and $\epsilon = \pi\hbar I/e$. The contribution F_G to the free energy due to regular configurations can be dropped, because it does not acquire an imaginary part under the analytic continuation. We now perform the analytic continuation $\tau \rightarrow it$, resulting in [see Ref. [29] for details]

$$\operatorname{Im} F = -\frac{Ly^2c_s^2}{2\kappa^4} \int_{-L/2}^{L/2} dx \int_{-\infty}^{\infty} dt e^{i\epsilon t - 2\mu g(x,t)}, \quad (5.3)$$

where $g(x,t) \equiv g_E(x,\tau \rightarrow it)$. The rate $\Gamma(\epsilon)$ then follows for $L, L_T \gg \kappa$ but arbitrary L/L_T in the form

$$\Gamma(\epsilon) = \frac{c_s^2 Ly^2}{\kappa^4} \int_{-L/2}^{L/2} dx \int_{-\infty}^{\infty} dt e^{i\epsilon t - \mu[\tilde{g}(t+x/c_s) + \tilde{g}(t-x/c_s)]},$$

where

$$\tilde{g}(t) = \ln[(L_T/\kappa) \sinh(\pi T|t|)] + i(\pi/2) \operatorname{sgn}(t).$$

Analyticity of $g_E(x,\tau)$ in the strip $0 \leq \tau \leq 1/T$ also leads to the standard detailed balance relation [29],

$$\Gamma(-\epsilon) = e^{-\epsilon/T} \Gamma(\epsilon).$$

In order to explicitly evaluate the rate $\Gamma(\epsilon)$ for arbitrary L/L_T , we now replace the boundaries for the x -integral by a soft exponential cutoff, switch to integration variables $t' = t - x/c_s$ and $t'' = t + x/c_s$, and use the auxiliary relation

$$e^{-c_s|t''-t'|/L} = \frac{c_s}{\pi L} \int_{-\infty}^{\infty} ds \frac{e^{-is(t''-t')}}{s^2 + (c_s/L)^2}.$$

The t', t'' time integrations then decouple, and it is straightforward to carry them out. Finally some algebra yields the linear resistance in the form

$$\begin{aligned} \frac{R(T)}{R_Q} &= \left(\frac{\pi y \Gamma(\mu/2)}{\Gamma(\mu/2 + 1/2)} \right)^2 \frac{\pi L}{2\kappa} \left(\frac{L_T}{\kappa} \right)^{3-2\mu} \\ &\times \int_0^{\infty} du \frac{2/\pi}{1+u^2} \left| \frac{\Gamma(\mu/2 + iuL_T/2L)}{\Gamma(\mu/2)} \right|^4, \end{aligned} \quad (5.4)$$

in units of the resistance quantum R_Q defined in Eq. (2.1).

For $L/L_T \gg 1$, the u -integral approaches unity, and hence $R \propto T^{2\mu-3}$, while for $L/L_T \ll 1$, dimensional scaling arguments give $R \propto T^{2\mu-2}$. In Refs. [3, 4], typical lengths were $L \approx 1 \mu\text{m}$, which puts one into the crossover

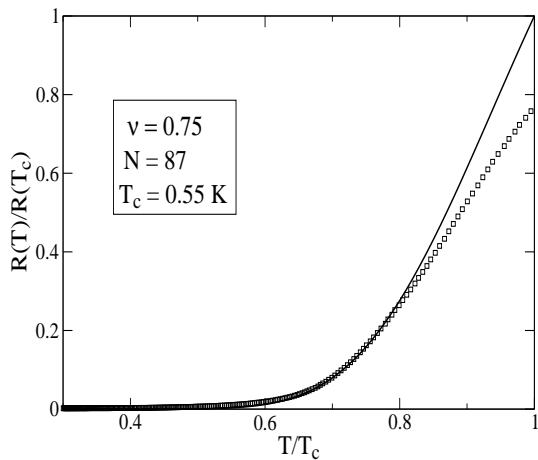


FIG. 3: Temperature dependence of the resistance below T_c for superconducting rope $R2$ experimentally studied in Ref. [4]. Open squares denote experimental data (with subtracted residual resistance), the curve is the theoretical result.

regime $L_T \approx L$. While the quoted power laws have already been reported for diffusive wires [15], Eq. (5.4) describes the full crossover for arbitrary L/L_T , and applies to strongly correlated ladder compounds such as nanotube ropes. It predicts that the transition gets significantly broader upon decreasing the number of tubes in the rope. This is shown in Fig. 2, where the theoretical results for the resistance is plotted for various N at $\nu = 1$. Note that Eq. (5.4) is a perturbative result in the fugacity, and it is expected to break down close to T_c , see below. In the next section we directly compare Eq. (5.4) to experimental data obtained by Kasumov *et al.* [4].

VI. COMPARISON TO EXPERIMENTAL DATA

Here we discuss how the prediction for the temperature-dependent resistance $R(T)$ below T_c as given in Eq. (5.4) compares to the experimental results for $R(T)$ published in Ref. [4]. More aspects of this comparison will be given elsewhere [30]. The experimental data in Ref. [4] were obtained from two-terminal measurements of ropes suspended between normal electrodes. Due to the presence of the contacts, the residual resistance (2.1) survives down to $T = 0$ even when the rope exhibits a superconducting transition. Extrapolation of experimental results for $R(T)$ yields R_c , which then allows to infer the number N in the respective sample from Eq. (2.1). This resistance R_c has to be subtracted from experimental data to allow for a comparison with Eq. (5.4), where no contact resistance is taken into account.

In Figs. 3 and 4, experimental resistance curves (after this subtraction) for the samples named $R2$ and $R4$ in Ref. [4] are plotted versus the prediction of Eq. (5.4). For sample $R2$, we find $R_c = 74 \Omega$ corresponding to $N_{R2} = 87$, while for sample $R4$, the subtracted resis-

tance is $R_c = 150 \Omega$, leading to $N_{R4} = 43$. We then take these N values when computing the respective theoretical curves. The experimentally determined temperature T^* locates the onset of the transition [4], and is identified with the true transition temperature T_c in Eq. (4.7). It is therefore also not a free parameter. Note that thereby the eigenvalue Λ_1 of the Josephson matrix has been determined. In the absence of detailed knowledge about the Josephson matrix, it is fortunate that our result for $R(T)/R(T_c)$ following from Eqs. (5.4) and (4.2) does not require more information about Λ besides the largest eigenvalue. Given the estimate $g_{c+} = 1.3$ [11], the comparison of Eq. (5.4) to experimental data then allows only one free fit parameter, namely ν . According to our discussion in Sec. IV A, the fit is expected to yield values $\nu \approx 1$.

The best fit to the low-temperature experimental curves for $R(T)$ yields $\nu = 0.75$ for sample $R2$, see Fig. 3, and $\nu = 0.16$ for sample $R4$, respectively. The agreement between experiment and theory is excellent for sample $R2$. For sample $R4$, the optimal ν is slightly smaller than expected, which indicates that dissipative processes may be more important in that sample. Nevertheless, for both samples, the low-temperature resistance agrees quite well, with only one free fit parameter that is found to be of order unity as expected. Whereas the agreement between theoretical and experimental curves appears then quite satisfactory in the low-temperature region, our predictions clearly deviate in the region near T_c . This is not surprising, because our expression for $R(T)$ in Eq. (5.4) is perturbative in the QPS fugacity. It is then expected to break down close to T_c , where QPSs proliferate and the approximation of a very dilute gas of QPS pairs, on which our calculation is based, is not valid anymore. As a consequence, also the saturation observed experimentally above T^* is not captured.

We note that it is an interesting challenge to compute the finite resistance in the normal phase at $T_c < T < T_c^0$, where the saturation should be caused by QPS and TAPS proliferation. For temperatures $T > T_c^0$, superconducting correlations can be neglected, and the resistance should then be dominated by phonon backscattering and disorder effects. Nevertheless, we believe that the agreement between the theoretical resistance result (5.4) and experimental data at low temperatures shown in Figs. 3 and 4, given the complexity of this system, is rather satisfactory. More importantly, this comparison provides strong evidence for the presence of quantum phase slips in superconducting nanotube ropes.

VII. CONCLUSIONS

According to our discussion above, the intrinsic superconductivity observed in ropes of SNWTs [3, 4] represents a remarkable phenomenon, where it has been possible to experimentally probe the extreme 1D limit of a superconductor. In this paper, we have formulated a the-

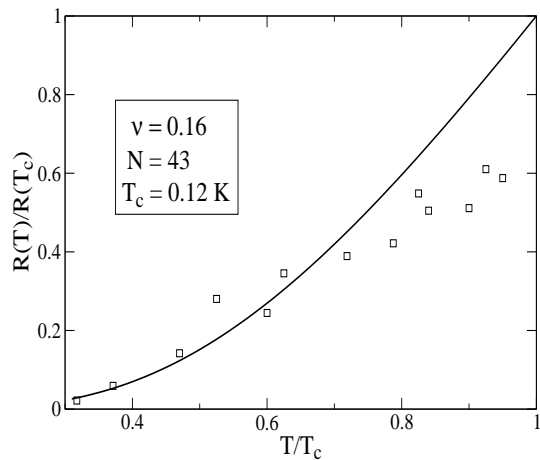


FIG. 4: Same as Fig. 3, but for sample *R4* experimentally studied in Ref. [4].

ory for this phenomenon, based on a model of metallic SWNTs with attractive intra-tube interactions and arbitrary inter-tube Josephson couplings. The analysis of this model leads to an effective Ginzburg-Landau action, whose coefficients can be expressed in terms of parameters entering the microscopic description of the rope. In order to get the correct low-energy dynamics, it is crucial to include quantum fluctuations of the order parameter.

Based on the resulting low-energy action for the phase fluctuations, we have shown that quantum phase slips produce a depression of the critical temperature. More importantly, the temperature dependence of the linear resistance experimentally observed below the transition temperature can be accounted for by considering the underlying LL physics and the effect of quantum phase slips. Despite some admittedly crude approximations, like the neglect of intra-tube disorder and dissipation effects inside the vortex core, the comparison of experimental curves and theoretical predictions, in particular in the low-temperature region, strongly suggests that the resistive process is indeed dominated by quantum phase slips. Our theory also suggests that, if repulsive Coulomb interactions can be efficiently screened off, superconductivity may survive down to only very few transverse channels in clean nanotube ropes.

Acknowledgments

We thank H. Bouchiat and M. Ferrier for providing the data shown in Figs. 3 and 4 and for many discussions. One of us (ADM) would like to thank them also for their warm hospitality during an extended stay in Orsay. This work has been supported by the EU network DIENOW and the SFB-TR 12 of the DFG.

-
- [1] C. Dekker, *Physics Today* **52(5)**, 22 (1999); See also reviews on nanotubes in *Physics World* No. **6** (2000).
- [2] M. Dresselhaus, G. Dresselhaus and Ph. Avouris (Eds.), *Carbon Nanotubes*, Topics in Appl. Physics **80** (Springer Verlag 2001).
- [3] M. Kociak, A.Yu. Kasumov, S. Gueron, B. Reulet, I.I. Khodos, Yu.B. Gorbatov, V.T. Volkov, L. Vaccarini, and H. Bouchiat, *Phys. Rev. Lett.* **86**, 2416 (2001).
- [4] A. Kasumov, M. Kociak, M. Ferrier, R. Deblock, S. Gueron, B. Reulet, I. Khodos, O. Stephan, and H. Bouchiat, *Phys. Rev. B* **68**, 214521 (2003).
- [5] Z.K. Tang, L. Zhang, N. Wang, X.X. Zhang, G.H. Wen, G.D. Li, J.N. Wang, C.T. Chan, and P. Sheng, *Science* **292**, 2462 (2001).
- [6] A.Yu. Kasumov, R. Deblock, M. Kociak, B. Reulet, H. Bouchiat, I.I. Khodos, Yu.B. Gorbatov, V.T. Volkov, C. Journet, and M. Burghard, *Science* **284**, 1508 (1999).
- [7] A.F. Morpurgo, J. Kong, C.M. Marcus, and H. Dai, *Science* **286**, 263 (1999).
- [8] C.N. Lau, N. Markovic, M. Bockrath, A. Bezryadin, and M. Tinkham, *Phys. Rev. Lett.* **87**, 217003 (2001).
- [9] J. González, *Phys. Rev. Lett.* **88**, 076403 (2002).
- [10] J. González, *Phys. Rev. B* **67**, 014528 (2003).
- [11] A. De Martino and R. Egger, *Phys. Rev. B* **67**, 235418 (2003).
- [12] A.A. Maarouf, C.L. Kane, and E.J. Mele, *Phys. Rev. B* **61**, 11156 (2000).
- [13] H.J. Schulz and C. Bourbonnais, *Phys. Rev. B* **27**, 5856 (1983).
- [14] M. Tinkham, *Introduction to Superconductivity*, 2nd ed. (McGraw-Hill, Inc., 1996).
- [15] A.D. Zaikin, D.S. Golubev, A. van Otterlo, and G.T. Zimanyi, *Phys. Rev. Lett.* **78**, 1552 (1997).
- [16] D.S. Golubev and A.D. Zaikin, *Phys. Rev. B* **64**, 014504 (2001).
- [17] H.P. Büchler, V.B. Geshkenbein, and G. Blatter, *Phys. Rev. Lett.* **92**, 067007 (2004).
- [18] J. González, *Eur. Phys. J. B* **36**, 317 (2003).
- [19] R. Egger and A.O. Gogolin, *Phys. Rev. Lett.* **79**, 5082 (1997).
- [20] C. Kane, L. Balents, and M.P.A. Fisher, *Phys. Rev. Lett.* **79**, 5086 (1997).
- [21] A.O. Gogolin, A.A. Nersesyan, and A.M. Tsvelik, *Bosonization and Strongly Correlated Systems* (Cambridge University Press, 1998).
- [22] R. Egger and A.O. Gogolin, *Eur. Phys. J. B* **3**, 281 (1998).
- [23] S.T. Carr and A.M. Tsvelik, *Phys. Rev. B* **65**, 195121 (2002).
- [24] Modes with $\Lambda_\alpha = 0$ have to be excluded in the transformation. All α summations have to be understood in this sense. Note that such modes never cause critical behavior in any case.
- [25] N. Nagaosa, *Quantum Field Theory in Condensed Matter Physics* (Springer Verlag, 1999).
- [26] J. E. Mooij and G. Schön, *Phys. Rev. Lett.* **55**, 114 (1985).
- [27] P.M. Chaikin and T. Lubensky, *Principles of Condensed Matter Physics* (Cambridge University Press, 2000).

- [28] J.S. Langer, *Ann. Phys. (N.Y.)* **41**, 108 (1967).
- [29] U. Weiss, *Quantum Dissipative Systems*, 2nd. ed. (World Scientific, Singapore, 1999).
- [30] M. Ferrier, A. De Martino, A. Kasumov, R. Deblock, S. Gueron, R. Egger, and H. Bouchiat, invited review, submitted to *Solid State Communications*.